

# Adaptive Hierarchical Decomposition of Large Deep Networks

Sumanth Chennupati\*, Sai Prasad Nooka\*, Shagan Sah, Raymond Ptucha  
*Rochester Institute of Technology, Rochester, New York 14623, USA*  
 {cv7148, spn8235, sxs4337, rupec}@rit.edu

Deep learning has recently demonstrated its ability to rival the human brain for visual object recognition. As datasets get larger, a natural question to ask is if existing deep learning architectures can be extended to handle the 50+K classes thought to be perceptible by a typical human. Most deep learning architectures concentrate on splitting diverse categories, while ignoring the similarities amongst them. This paper introduces a framework that automatically analyzes and configures a family of smaller deep networks as a replacement to a singular, larger network. Class similarities guide the creation of a family from coarse to fine classifiers which solve categorical problems more effectively than a single large classifier. The resulting smaller networks are highly scalable, parallel and more practical to train, and achieve higher classification accuracy. This paper also proposes a method to adaptively select the configuration of the hierarchical family of classifiers using linkage statistics from overall and sub-classification confusion matrices. Depending on the number of classes and the complexity of the problem, a deep learning model is selected and the complexity is determined. Numerous experiments on network classes, layers, and architecture configurations validate our results.

*Keywords:* Hierarchy; Decomposition; Image Classification; Multi-layer Perceptron; Convolutional Neural Network.

## 1. Introduction

We carry in our heads a marvel of the universe, tuned by evolution over millions of years. In each hemisphere of our brain, the primary visual cortex contains 140 million neurons, each connecting with up to ten thousand other neurons, forming a massive network with tens of billions of connections. And yet, human vision involves not just  $V1$ , but an entire series of visual cortices -  $V2$ ,  $V3$ ,  $V4$ , and  $V5$  each doing progressively more complex visual processing. Recognizing objects isn't easy. Rather, we humans are stupendously, astoundingly good at making sense of what our eyes show us.

Teaching computers how to perform such object recognition is a challenging task. Convolutional Neural Networks ( $CNNs$ ) offer solutions to such highly complex object recognition challenges and have revolutionized the fields of computer vision and pattern recognition. With respect to object detection,  $CNNs$  have demonstrated extraordinary performance on the 1000-class ImageNet<sup>5</sup> dataset, recently surpassing human-level performance<sup>10,31</sup>. Although  $CNNs$  have been trained for

\*Equal Contribution

upwards of  $10K$  classes, the number of weights in the fully connected layers grow exponentially, demanding a daunting number of training samples, and consuming huge computational resources.

Deep architectures<sup>16,27,32,31,9</sup> with hierarchical frameworks enable the representation of complex concepts with fewer nodes than shallow architectures. AlexNet<sup>16</sup>, VGG<sup>27</sup> and GoogLeNet<sup>32</sup> are large, deep convolutional neural networks, trained on 1.2 million high-resolution images and 1000 classes in the ImageNet Large Scale Visual Recognition Competition (ILSVRC 2010). It has been shown that network depth is more important than the number of nodes in each layer<sup>22</sup>, with modern architectures containing over 100 layers<sup>31,9</sup>, requiring the solution of over  $100M$  parameters.

As the classification task becomes more difficult, the number of parameters increases exponentially, making the classification not only difficult to train but more likely to overfit the data. It is clear that if number of parameters in a network is too large then the network will try to memorize the patterns rather than trying to generalize the training data. Techniques such as domain adaptation<sup>13</sup> and hashing<sup>3</sup> have been used to tackle problems with larger classes. Yan et al.<sup>37</sup> leveraged the hierarchical structure of categories by embedding *CNNs* into category hierarchies.

This paper introduces a multi-layer hierarchical framework to reduce the overall number of solvable parameters by subdividing the classification task into smaller intrinsic problems. Abstract higher level networks initially determine which sub-network a sample should be directed to, and lower level networks take on the task of finding discriminating features amongst similar classes. Each sub-network is called a class assignment classifier and can recursively be split into subsequently smaller classifiers. Outputs from these class assignment classifiers predict a test samples final class.

Confusion matrices infer class-wise linkage statistics by converting from similarity to dissimilarity matrices. Similarly, k-means and spectral clustering on low dimensional representations of the data offer clues to natural boundaries at a coarser level. By viewing the resulting graph tree, such as a dendrogram graph, logical cluster boundaries can often be determined by manual inspection. Data driven heuristics along with an iterative search algorithm can automatically detect cluster boundaries. These statistics form a hierarchical representation where classes with different superclass labels exhibit dissimilar features at a higher level and classes with same superclass label (i.e, subclasses) share similar features at lower level. These subclasses belong to a cluster that feed an independent class assignment classifier. To ensure robustness and improved generalization, classes which share similarities across different clusters are encouraged to have multiple superclass labels. Semantic outputs from the activated class assignment classifiers include softmax probabilities. The outputs of the classifiers, feed a final classification engine, which makes the final class decision.

The size and type of architecture of a deep network can have a profound impact on both network accuracy and training resources. Considering the importance of

appropriate network configuration for classification tasks, we propose an adaptive network selection approach. The clusters generated during hierarchical clustering exhibit different properties. Classes in these clusters have different statistical characteristics and levels of confusion. Adaptive network configurations should examine the confusion among the subclasses and decide an appropriate network configuration to optimize these individually.

In addition to introducing automated methods for automatically choosing adaptive network configurations, we demonstrate the advantages of using transfer learning as an initialization for the class assignment classifier rather than training an entire network from scratch. Adaptive models determine whether it is best to use pre-trained networks as an initialization or as a fixed feature extractor for each of the families of networks.

In this paper we make the following contributions: (1) a framework that automatically analyzes and configures a family of smaller deep networks as a replacement to a singular, larger network, (2) resulting smaller networks are not only highly scalable, parallel and more practical to train, but also achieve higher classification accuracy, (3) a method to adaptively select the configuration of the hierarchical family of classifiers.

## 2. Background

The pioneering work of Hubel and Wiesel<sup>15</sup> laid the foundation for the modern hierarchical understanding of the ventral stream of the primate visual cortex. Simple receptive fields in the eye form complex cells in V1, then more abstract representations in V2 through V4, and finally into the inferior temporal (IT) cortex. The object representation in the IT cortex is amazingly robust to position, scale, occlusions, and background- the exact understanding of which still remains a mystery and marvel of the human brain<sup>17</sup>.

Traditional computer vision techniques pair hand crafted low level features such as SIFT<sup>20</sup>, SURF<sup>1</sup>, or HOG<sup>2</sup> along with complimentary classifiers such as support vector machines (SVM) or neural networks. LeCun et al.<sup>18</sup> introduced convolutional neural networks (*CNNs*), computer vision oriented deep feed forward networks based upon a hierarchy of abstract layers. *CNNs* are end-to-end models, learning the low level features and classifier simultaneously in a supervised fashion, giving substantial advantage over methods using independent vision features and classifiers.

Datasets such as MNIST<sup>18</sup>, CalTech<sup>6</sup>, and Pascal<sup>39</sup> have become more challenging over the years. The ImageNet<sup>5</sup> dataset has over 14M images from over 20,000 categories. In 2012, Krizhevsky and Hinton<sup>16</sup> beat the nearest competitor by 10% in the ImageNet Large-Scale Visual Recognition Challenge (ILSVRC)<sup>25</sup> competition with a seven layer deep *CNN*, taking advantage of a powerful regularization scheme called dropout<sup>28</sup>.

Recent progress in classification accuracy can be attributed to advances in build-

ing deeper architectures and improved regularization methods<sup>28,8,34,12</sup>. Zeiler & Fergus<sup>38</sup> improved classification results by introducing random crops on training samples and improved parameter tuning methodologies. Simonyan and Zisserman<sup>27</sup> investigated the usage of network depth and Szegedy, et al.<sup>32</sup> used banks of smaller convolutional filters to simultaneously improve accuracy while decreasing the number of parameters. Zhang, et al.<sup>11</sup> computed the feature maps from the entire image only once, and then pooled features in arbitrary regions (sub-images) to generate fixed-length representations.

Other advances are attributed to the use of new non-linear activations<sup>8,21,23,19,30</sup> such as Rectifier Linear Units (ReLU). Zhang, et al. He, et al.<sup>10</sup> used a parameterized version of ReLU to simultaneously learn slope parameters along with weight hyper parameters during backpropagation.

There are numerous works describing hierarchical decomposition of classification problems<sup>33</sup>. One of the earliest attempts of a *CNN* hierarchical approach<sup>29</sup> used transfer learning from clusters with many samples to clusters with few. Deng et al.<sup>4</sup> used a hierarchy of label relations, and further improvements were made by<sup>35,37</sup> using two and many categories, respectively.

To form class clusters, confusion matrices can be used to determine hierarchical clusters<sup>7,24,36</sup> increased robustness by allowing classes to fork in more than one hierarchical branch. Salakhutdinov et al. Salakhutdinov, et al.<sup>26</sup> combined structured hierarchical Bayesian models with deep learning to generate a framework that can learn new concepts with a minimal number of training samples. *CNN* hierarchical improvements were demonstrated by<sup>32,14</sup> and a category hierarchical *CNN* based classifier, *HD-CNN*, was demonstrated in<sup>37</sup> but the memory footprint and time constraints were the major challenges. In<sup>37</sup> the synsets of ImageNet are used for the coarse category taxonomy. These coarse categories or the taxonomy is automatically built using spectral clustering or linkage statistics. The *HD-CNNs* in<sup>37</sup> used pre-training for individual classifiers and fine tune them with end to end training. During testing, *HD-CNN* uses all classifiers to make a final class estimation. This requires more computations and memory compared to our proposed model which requires only a single classifier to make the final class estimation.

### 3. Methods

We propose a novel method to alleviate the computational complexity involved in training larger networks on datasets with higher number of discrete classes or concepts. Our approach (shown in Fig. 1) uses a high-level classifier to initially determine which cluster a sample belongs to, and then passes that sample into the corresponding class assignment classifier to make the final class assignment. Moreover, the optimal number of clusters are automatically determined and each subclass is trained independently. The first stage is hierarchy clustering for determining the number of clusters. This exploits the rich information from a class-to-class confusion matrix (generated using a simplified conventional neural network mapping to all

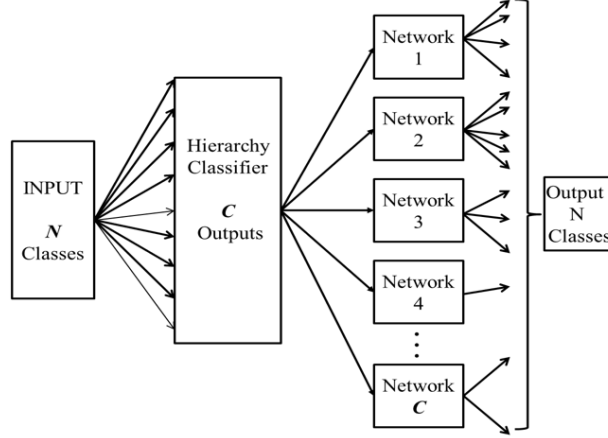


Fig. 1. Illustration of hierarchical deep network framework.

classes or concepts) to find hidden correlations amongst classes and form clusters. After the initial training, the hierarchy classifier predicts a cluster for each sample. This sample is passed into one of  $C$  smaller class assignment classifiers, each of which is only concerned with a subset of classes to make a final classification estimate. The approach can be divided into three phases (shown in Fig. 2): (1) hierarchical clustering, (2) hierarchy classifier, and (3) class assignment classifiers. In the following sub-section we will describe each of these modules in detail.

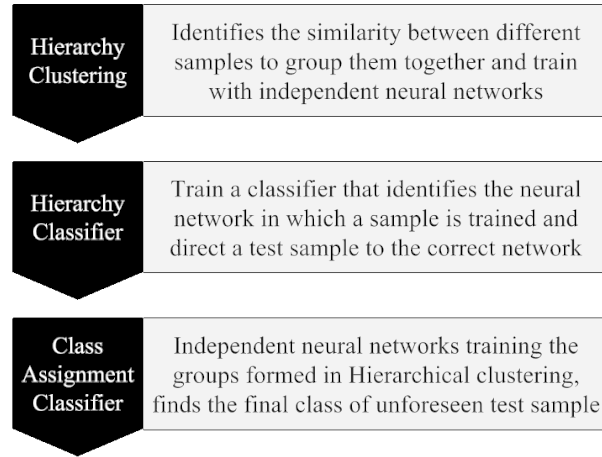


Fig. 2. Flow of classification using hierarchical deep networks.

### 3.1. *Hierarchy Clustering*

To address classification problems with very large number of classes, we propose a hierarchical approach for clustering similar classes into clusters. This requires training of a handful of much simpler neural networks with a reduced number of overall parameters. The intuition for using a hierarchical clustering is the presence of coarse categories or super classes that comprise of a higher number of fine classes. To generate clusters from a given set of classes, we perform spectral clustering on the confusion matrix. The main challenge with such a hierarchical clustering scheme is the selection of an optimum merge or split breakpoints, which if done improperly, can lead to low quality clusters. To address this issue, we formulate an automated multi-phase technique that is based on the analysis of the class confusion matrix of the classifier in the parent stage.

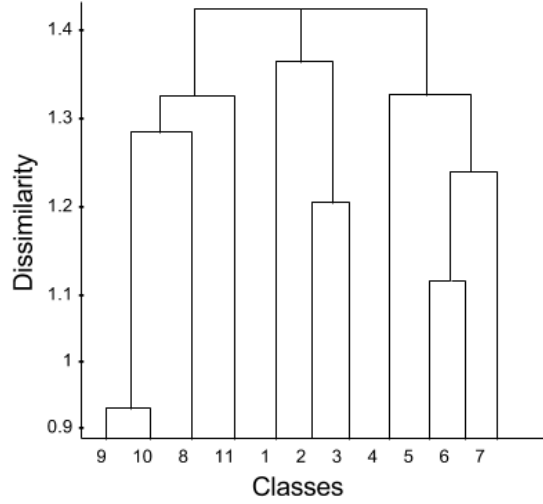
We use the linkage statistics from a class confusion matrix for getting correlation indicators among classes in a hierarchical configuration. The distance matrix ( $D$ ) is estimated from the class confusion matrix ( $C$ ), and measures the dissimilarity among different classes.  $D$  is computed by a simple three step process: (i) transform similarity to dis-similarity  $D = 1 - C$ , (ii) set self dis-similarity to zero  $D_{ii} = 0$ , and (iii) make the matrix symmetric  $D = 0.5 * (D + D^T)$ . In this paper,  $C_i$  represents class  $i$  and  $Q_i$  represents cluster  $i$ .  $D_p(C_i, C_j)$  represents the dissimilarity between Classes  $C_i$  and  $C_j$  and  $D_p(Q_i, Q_j)$  represents the dissimilarity between clusters  $Q_i$  and  $Q_j$ .

In order to create coarse and fine categories (shown in Fig. 4), a multi-stage iterative process is deployed to sub-divide the parent cluster into smaller class clusters until a termination criterion is met. In a stage  $p$ ,  $D$  will have dimensions  $K_p \times K_p$ , where an element  $D_p(Q_i, Q_j)$  represents the dissimilarity between clusters  $i$  and  $j$ . An unweighted pair cluster method based on the arithmetic mean is used for determining the linkages between individual clusters.  $D_p(Q_i, Q_i) = 0 \ \forall i \in K$ , represents the dissimilarity of a cluster with itself. We use a top-down divisive strategy to find non-overlapping classes that starts by including all classes in a single cluster. The dissimilarity between clusters dynamically determines the split points with an upper limit on the number of classes in a cluster. As a result, this technique automatically adapts to the internal characteristics of the data. This is one of the most important advantages with using such an approach that adapts to the dataset.

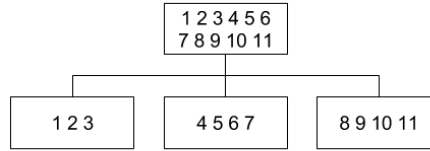
Small non-overlapping clusters are obtained by clustering similar classes together. However, during test time in a non-overlapping setting, a misclassified sample at a parent level would always be predicted incorrectly at the lower levels. Therefore to achieve a higher generalization, classes in smaller clusters are overlapped using the posterior probabilities. The confusion matrix of the parent cluster are column normalized  $DCN_p$  to obtain the class posterior probabilities. An element  $DCN_p(C_i, C_j)$  represents the likelihood that a sample is of the true class  $C_i$  given that it was predicted as class  $C_j$ . Let cluster  $Q_i$  be the collection of classes

$C_{i,\dots,n}$ , then the condition that a certain class  $C_j$  is similar to this cluster  $Q_i$  can be given as,

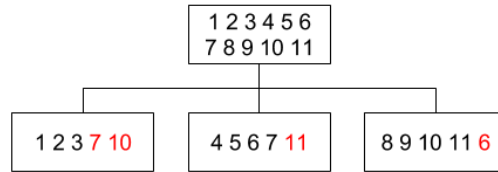
$$DCN_p(C_i, C_j) \geq (\gamma \cdot K_{p-1})^{-1} \quad \forall C_i \in Q_i, C_j \notin Q_i \quad (1)$$



(a) Example of a dendrogram with dissimilarity among the classes.



(b) Example of the non-overlapping clusters formed.



(c) Example of the overlapping clusters.

Fig. 3. Illustration of hierarchy clustering on Toy data having 11 classes.

We use a parametric threshold of  $(\gamma \cdot K_{p-1})^{-1}$ , where  $\gamma$  is an overlapping hyper-

parameter that determines the probability for including a class  $C_j$  in cluster  $Q_i$ . The value of  $\gamma$  depends on the number of classes in the original problem and the number of clusters in the parent stage. Since the clustering is done in a hierarchical fashion, the threshold is dependent on the number of classes in the previous stage ( $K_{p-1}$ ). Thus, all classes that are not a part of cluster  $Q_i$  are compared with the cluster. The overlapping in the classifier allows a test sample to follow multiple paths of sub-classifiers. Algorithm 1 describes the pseudo code of the class clustering algorithm.

---

**Algorithm 1** Hierarchy Class Clustering

---

Hierarchy relationships between classes are derived using the confusion matrix  $C_p$  that measures linkage distances  $d$  between classes. To form clusters with overlapping classes, we threshold class posterior probabilities  $DCN$  for classes originally not in cluster.

**Input:** Confusion matrix  $C_p$  at classification stage  $p$

**Output:** Overlapping class labels  $Q$

**Initialize:** Upper limit on non-overlapping cluster size and overlapping factor  $\gamma$

- 1: Compute distance matrix  $D$  from  $C_p$
  - 2: Compute linkage statistics:
$$d(r, s) = \frac{1}{n_r \cdot n_s} \sum_{i=1}^{n_r} \sum_{j=1}^{n_s} dist(x_{r_i}, x_{s_j})$$

Where  $x_{r_i}$  and  $x_{s_j}$  are dissimilar clusters with  $n_r$  and  $n_s$  elements, respectively
  - 3: Compute cumulative linkage values  $Cum(d)$ 
    - for** descending values  $k$  in  $Cum(d)$ 
      - $\alpha$  = no. of classes with  $d < k$
      - if**  $\alpha > \theta$  **then**
        - cluster classes  $\alpha$  as a new cluster  $Q$
    - end**
  - 4: Compute column normalized confusion matrix ( $DCN$ )
    - for** each cluster  $Q_i$ 
      - if**  $DCN_p(C_i, C_j) \geq (\gamma \cdot K_{p-1})^{-1} \forall C_i \in Q_i, C_j \notin Q_i$  **then**
        - append class  $j$  to cluster  $Q_i$
    - end**
- 

### 3.2. Hierarchy Classifier

Let  $S$  be the training set with  $N$  classes, where  $C$  clusters are formed after hierarchical clustering, such that  $C$  clusters have  $n_1, n_2, n_3 \dots n_c$  number of classes and  $n_1 + n_2 + n_3 + \dots + n_c = N$ . The linkage statistics define a high-level classifier, called the hierarchy classifier, which determines the cluster a sample belongs to. Samples are passed into the corresponding sub-class network to make the final class assign-



ment. These subclass networks are referred to as class assignment classifiers.

### 3.3. Class Assignment Classifier

The class assignment classifier consists of  $C$  smaller neural networks, each predicting a unique and inclusive subset of the  $N$  classes. Each of the  $C$  class assignment classifiers output their respective subset of  $N$  classes, i.e., all classes of the dataset are classified at this stage of hierarchical model. In order to mitigate misclassifications from the previous stage of hierarchy classifier during testing, overlapping clusters allow a sample to pass to more than one class assignment classifier. Let  $p_1, p_2, p_3, \dots, p_c$  be predictions of the hierarchy classifier for corresponding  $C$  outputs and  $q_1, q_2, q_3, \dots, q_c$  be the predictions of  $Network_1$  for the corresponding  $n_1$  outputs. The top  $k$  predictions from overlapping clusters are predictions of the hierarchy classifier and the class assignment classifier. The final predicted classification output is referred as confidence ( $\mathcal{C}$ ):

$$Confidence(\mathcal{C}_i) = p_j \times q_k \forall i \in (1, C), k \in (1, n_j) \quad (2)$$

To boost the performance of hierarchical models, this study introduces an adaptive network selection manager as shown in Fig. 4. The network selection manager considers both the number of classes as well as cluster heuristics to select an appropriate network configuration for each class assignment classifier. Experiments determine the best configuration for a given cluster. A CNN with a preset number of layers and filters is used as a base configuration and the adaptive network model determines the configuration used for any cluster.

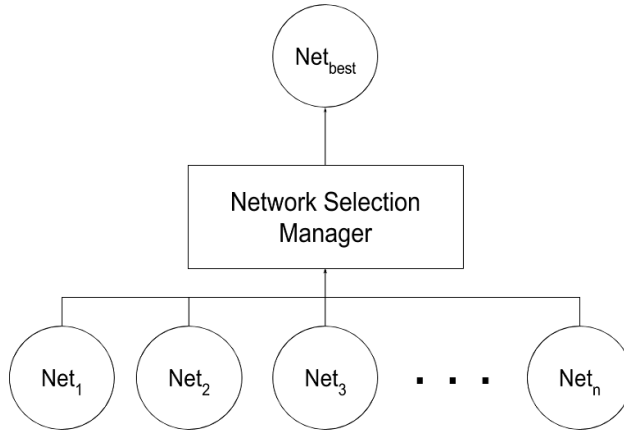


Fig. 4. Illustration of a network selection manager that chose between  $n$  different networks.

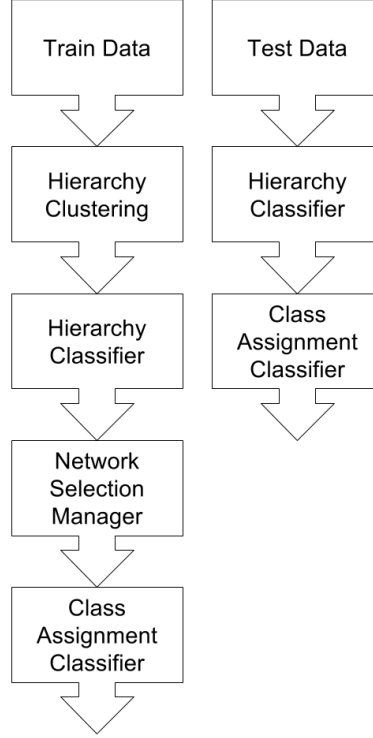


Fig. 5. Illustration of updated hierarchical model with Network selection manager.

Fig. 5 shows the stages of an adaptive hierarchical model. It includes a network selection manager that selects the best network configuration for the class assignment classifier. During training, the hierarchy classifier predicts a cluster a sample belongs and passes it through one of  $C$  smaller class assignment classifiers that are chosen by the network selection manager.

The following sections will discuss the adaptive network selection strategy and the adaptive transfer learning variants of the network selection manager.

### 3.4. Adaptive Network Selection

The number of layers in the network and number of nodes per layer are both important in optimizing classification problems. Since hierarchical clusters exhibit unique statistical properties, selecting an appropriate network would typically improve the overall classification accuracy. Attributes such as the number of classes, confusion matrix linkage and class-to-class correlation statistics allow an adaptive network framework to make the classifier decision. It selects a network from a set of pre-configured CNN architectures shown in Tables 1 & 2 which vary in number of layers

and nodes/filters per layer. Rather, for Multi-Layer Perceptrons (*MLPs*) the decision on network architecture- layers and number of nodes, for a cluster is treated as a regression problem.

To train such a regressive model, multiple network configurations were trained on different clusters, where each cluster has its unique statistical properties. The model learns to correlate cluster properties with the corresponding best network architecture. This regression model provides 2 outputs for *MLPs* : 1) number of layers required, 2) Number of neurons required in each layer.

---

**Algorithm 2** Adaptive Network Selection

---

The network selection manager outputs the best network configuration for a class assignment classifier based on cluster heuristics.

**Input:** Non- Overlapping class labels  $C$  or Overlapping class labels  $Q$

**Output:** Best network configuration  $Net_{best}$

**Initialize:**  $Net_{best} = Net_1$

- 1: Send this cluster into pre-defined classifier and generate confusion matrix  $CM$ .
  - 2: Change the number of nodes in the final layer of the pre-defined networks ( $Net_1, Net_2, Net_3, \dots, Net_n$ ) to classify all subclasses in  $C$  or  $Q$ .
  - 3: Evaluate accuracy  $\mathcal{A}_i$  over all samples that contain class labels  $C$  or  $Q$ .
 

**for** all networks  $Net_i$  in  $Net_1, Net_2, Net_3, \dots, Net_n$ 

$\mathcal{A}_i = \text{Accuracy of network } Net_i \text{ for all samples with subclass labels in } C \text{ or } Q.$

**if**  $\mathcal{A}_i > \mathcal{A}_{best}$  **then**

$Net_{best} = Net_i$

repeat until all networks are evaluated.
  - 4: Pile up the dataset using the best network as label and features as confusion matrix  $CM$
  - 5: Depending upon *MLPs* or *CNNs* used, regression or classification networks are trained using the above generated dataset.
- 

### 3.5. Adaptive Transfer Learning

*CNNs* learn to extract features along with a feature classifier for unsurpassed image classification performance. It has also been widely shown that transfer learning enable both higher classification accuracies and faster convergence when applied to new classification problems. For example, the popular architectures of AlexNet<sup>16</sup>, VGG<sup>27</sup>, and GoogLeNet<sup>32</sup> that are pre-trained on ImageNet offer an excellent weight initialization for new visual classification problems. The first few layers of *CNNs* describe high level abstract features which apply equally to most visualization problems, negating the need for further fine-tuning. Initializing all weights from a

previously learned network and fine-tuning last few layers typically offers increased performance. Furthermore, such an initialization requires only a few training epochs are required for converge. Experiments demonstrate the impact that transfer learning has on the adaptive architectural selection.

### 3.6. Joint Model

In earlier sections, either convolutional neural networks or multi-layer perceptron neural networks in an adaptive mode are used. We now allow this selection in conjunction to select the optimum model configuration for a particular sub-network.

## 4. Experiments & Results

Several experiments were performed to demonstrate the application of the hierarchical models and adaptive hierarchical models. Multiple architectures were carefully pre-defined to feed the network selection manager which selects the best possible network for different class assignment classifiers. The CalTech-101, CalTech-256, CIFAR-100, ImageNet100, ImageNet200 and ImageNet datasets were used. The CalTech-101 dataset has 102 classes, with 40 to 800 images per class with image size of  $300 \times 200 \times 3$  pixels. The CalTech-256 dataset has 257 classes, with 80 to 827 images per class with image size of  $300 \times 200 \times 3$  pixels. These images were resized to  $64 \times 64$ . Training and testing splits for CalTech datasets were generated using 6-fold cross validation. The CIFAR-100 dataset has 100 classes with 500 images for training and 100 images for testing respectively per class and has an image size of  $32 \times 32 \times 3$  pixels. CIFAR-100 consists of 100 fine categories and 20 coarse categories with  $32 \times 32$  RGB images. ImageNet dataset has 1000 classes with 1350 samples per class and images are resampled to  $224 \times 224$  RGB images for all experiments in this paper. ImageNet100 and ImageNet200 are subsets of ImageNet with 100 and 200 classes randomly selected from the 1000 classes.

### 4.1. Training

For all experiments in this paper baseline CNN configuration refers to  $CNN_1$  from the pre-defined configurations described in Table 1. For all transfer learning experiments  $CNN_{TL_1}$  refers to baseline. The pre-defined CNNs,  $CNN_2$  through  $CNN_5$ , each contain six layers, the first four being convolution layers followed by pooling and the final two are fully connected layers with a dropout ratio of 0.5. Conv  $5 \times 5|32$  Stride:4 indicates convolutional operation with 32 filters of size of  $5 \times 5$  with a stride factor 4. ReLU, Maxpool|2 allows convolutional output to non-linear activation function followed by maxpooling with stride 2.  $FC$  is the number of nodes in the fully connected layer. All networks are trained for 40 epochs with a learning rate 0.01 and momentum 0.9. The adaptive transfer learning configurations,  $CNN_{TL_2}$  through  $CNN_{TL_5}$ , each contain 7 weight layers of which the first five are convolution layers and rest are fully connected layers with the same dropout ratio of 0.5.  $CNN_{TL_1}$  is identical to the VGG-f configuration<sup>27</sup>.

Table 1. Pre-defined convolutional neural network configurations for CalTech-101, CalTech-256.

Net	$CNN_1$	$CNN_2$	$CNN_3$	$CNN_4$	$CNN_5$
Depth	6	6	6	8	10
	Input: $64 \times 64$ RGB image				
Conv	$5 \times 5 32$	$3 \times 3 32$	$7 \times 7 32$	$5 \times 5 32$	$5 \times 5 32$
	ReLU, Maxpool 2				
Conv	$5 \times 5 32$	$3 \times 3 32$	$5 \times 5 32$	$3 \times 3 32$	$3 \times 3 32$
	ReLU, Maxpool 2				
Conv	$5 \times 5 64$	$3 \times 3 64$	$3 \times 3 64$	$3 \times 3 32$	$3 \times 3 32$
	ReLU, Maxpool 2				
Conv	$5 \times 5 64$	$3 \times 3 64$	$3 \times 3 64$	$3 \times 3 64$	$3 \times 3 64$
	ReLU, Maxpool 2				
FC	1024	512	256	512	512
	ReLU, Dropout				
FC	512	256	128	128	256
	ReLU, Dropout				
FC	C	C	C	C	C

#### 4.1.1. Hierarchical Model

The hierarchical model consists of a hierarchical classifier which makes coarse category predictions and a class assignment classifier that predicts the final class category of a test image. In a simple hierarchical model, a sample with its coarse category label is sent to a hierarchical classifier which learns the coarse category representations present in the dataset. Later, the sample is sent to one of the class assignment classifiers based on the fine category label. This allows the hierarchical model to learn the coarse and fine category representations in the dataset and effectively use them to make final predictions.

In the MLP experiments, a single large network contains 2 hidden layers with dimensions [200, 150] and a hierarchical classifier, while class assignment classifiers use a network with 2 hidden layers of size [25, 10]. For experiments with the CNNs, networks described in Table 1.  $CNN_2$  and  $CNN_3$  are used as hierarchical and class assignment classifiers respectively for CalTech-101 and CalTech-256 datasets. For CIFAR-100, the last layer of all the networks is replaced to fit the number of classes.

#### 4.1.2. Adaptive Hierarchical Model

Adaptive hierarchical model slightly differs from the hierarchical model in the second stage of classification where a sample is processed for fine category prediction. In the training phase, a sample directed towards a class assignment classifier is sent to all pre-defined networks and the best model is selected by the network selection manager that is later used in the testing phase to make fine category predictions.

In experiments with MLPs, several combinations of networks were used as described in section 3.4 and the resulting regression model was used to predict the class assignment classifier for the testing phase. In experiments with CNNs, information from  $CNN_2$  through  $CNN_5$  was used by the network selection manager to select the best network configuration for a given cluster.

#### 4.1.3. Adaptive Transfer Learning

In the hierarchical experiments on ImageNet dataset, we used  $CNN_{TL_1}$  as the base model,  $CNN_{TL_3}$  for making coarse category predictions and  $CNN_{TL_5}$  for making fine category predictions. For adaptive transfer learning, adaptive network section manager chooses between  $CNN_{TL_2}$  through  $CNN_{TL_5}$  from Table 2. Layers in blue are optimized by fine tuning and all other layers are fixed. Pre-trained weights for transfer learning experiments are obtained from VGG<sup>27</sup> that was trained on ImageNet dataset for 20 epochs.

Table 2. Pre-trained configurations for ImageNet datasets.

Net	$CNN_{TL_1}$	$CNN_{TL_2}$	$CNN_{TL_3}$	$CNN_{TL_4}$	$CNN_{TL_5}$
Depth	8	8	8	8	8
	Input: $224 \times 224$ RGB image				
Conv	$11 \times 11 64$ Stride:4	$11 \times 11 64$ Stride:4	$11 \times 11 64$ Stride:4	$11 \times 11 64$ Stride:4	$11 \times 11 64$ Stride:4
	ReLU,Maxpool 2				
Conv	$5 \times 5 256$	$5 \times 5 256$	$5 \times 5 256$	$5 \times 5 256$	$5 \times 5 256$
	ReLU,Maxpool 2				
Conv	$3 \times 3 256$	$3 \times 3 256$	$3 \times 3 256$	$3 \times 3 256$	$3 \times 3 256$
	ReLU				
Conv	$3 \times 3 256$ $3 \times 3 256$	$3 \times 3 256$ $3 \times 3 256$	$3 \times 3 256$ $3 \times 3 256$	$3 \times 3 256$ $3 \times 3 256$	$3 \times 3 256$ $3 \times 3 256$
	ReLU,Maxpool 2				
FC	4096	4096	2048	2048	1024
	ReLU, Dropout				
FC	4096	2048	2048	1024	1024
	ReLU, Dropout				
FC	$C$	$C$	$C$	$C$	$C$

## 4.2. Results

Table 3. demonstrates that a MLP processing on the CalTech-101 dataset increases the final accuracy by approximately 16% using a non-overlapping hierarchical architecture. Similar observations were recorded with overlapping hierarchical architecture, but performance decreases with increasing overlap factor. This was attributed to the increase in confusion in the hierarchical stage. It should also be noted that

the memory requirements increase as the overlap factor increases due to larger class assignment classifiers.

Table 3. Performance of hierarchical models built using MLPs on CalTech-101 dataset.

C	Clustering Method	Gamma( $\gamma$ )	HC(%)	FC(%)
1	NA	NA	NA	45.6
44	Non-Overlap	NA	69.43	61.39
44	Overlap	3	69.05	<b>61.56</b>
44	Overlap	5	62.73	60.13
44	Overlap	8	52.05	58.61

*Note:* Top line indicates performance of a single large MLP neural network with two hidden layer of dimensions [200, 150]. MLP neural network with two hidden layers of dimensions [25, 10] used in each mini-network for the rest of the models. Hierarchical clustering is controlled by varying the parameter gamma ( $\gamma$ ). *HC* indicates hierarchy classifier accuracy and *FC* indicates final classification accuracy.

In Table 4., evaluation using CNNs decreased the final accuracy by 4% when using a non-overlapping hierarchical architecture. Potential reasons explaining this decline are 1) the identical architecture of all the mini-networks, and 2) when a cluster has fewer number of classes, the number of training samples for that network are also less, making them insufficient for training CNNs.

Table 4. Performance of hierarchical models built using CNNs on CalTech-101 dataset.

C	Clustering Method	Gamma( $\gamma$ )	HC(%)	FC(%)
1	NA	NA	NA	55.84
48	Non-Overlap	NA	62.42	51.57
48	Overlap	3	50.33	50.72

*Note:* Top line indicates performance of a single large CNN. Similar CNNs are used in each mini-network of other experiments.

Table 5 & Table 7 show that the accuracy increases by 3% in cases of CalTech-256 and CIFAR-100 datasets when MLP neural network was used to evaluate the performance of the non-overlapping and overlapping hierarchical architectures. Table 6 & Table 8, show that final accuracy decreased when using CNNs to evaluate CalTech-256 and CIFAR-100 datasets. This can be attributed to the issue with smaller sized clusters as explained earlier.

The dendrograms in Fig. 6(a), 6(b), 7(a), 7(b), represent the class clustering

Table 5. Performance of hierarchical models built using MLPs on CalTech-256 dataset.

C	Clustering Method	Gamma( $\gamma$ )	HC(%)	FC(%)
1	NA	NA	NA	18.61
104	Non-Overlap	NA	23.07	21.56
104	Overlap	3	24.49	21.96
104	Overlap	5	22.55	20.61

Table 6. Performance of hierarchical models built using CNNs on CalTech-256 dataset

C	Clustering Method	Gamma( $\gamma$ )	HC(%)	FC(%)
1	NA	NA	NA	36.21
104	Non-Overlap	NA	29.87	28.34
104	Overlap	3	30.65	25.62
104	Overlap	5	27.38	21.47

Table 7. Performance of hierarchical models built using MLPs on CIFAR-100 dataset.

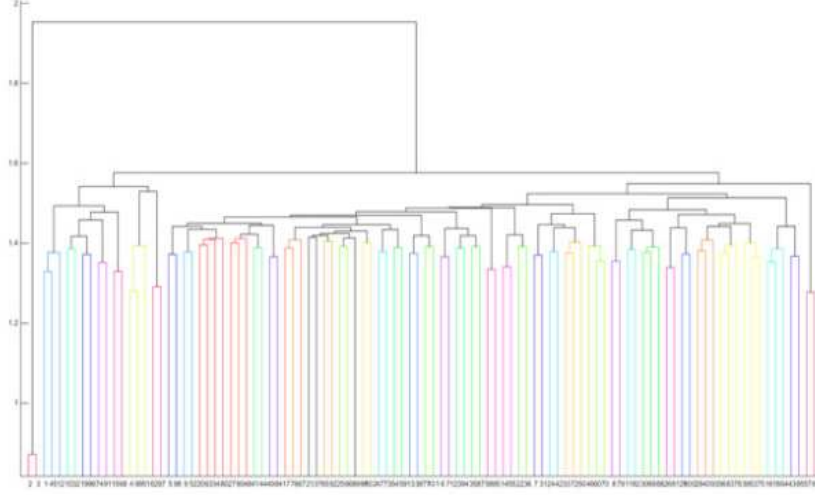
C	Clustering Method	Gamma( $\gamma$ )	HC(%)	FC(%)
1	NA	NA	NA	22.83
30	Non-Overlap	NA	28.37	24.96
30	Overlap	3	27.89	24.82
30	Overlap	5	26.34	23.25

Table 8. Performance of hierarchical models built using CNNs on CIFAR-100 dataset.

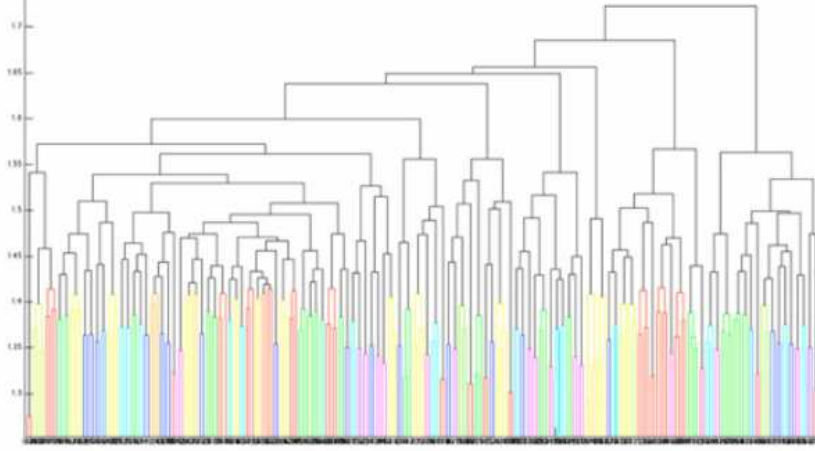
C	Clustering Method	Gamma( $\gamma$ )	HC(%)	FC(%)
1	NA	NA	NA	22.83
30	Non-Overlap	NA	28.37	24.96
30	Overlap	3	27.89	24.82
30	Overlap	5	26.34	23.25

formed using the linkage statistics for different data sets. The colors in the graph depict class clusters as determined by the algorithm described in Algorithm. 1. The height of the bars represent the magnitude difference between the clusters. It shows the decomposition of the clusters from a top-down perspective on different datasets. For example, Fig. 6(a) shows that the first two classes on the left are different from the remaining classes of the CalTech-101 dataset. The relatively flat joining lines in 7(b) along the top are indicative of a fairly balanced dataset. Further manual analysis of the clusters indicate that the that similar classes were clustered together which proves the efficacy of the hierarchical clustering.





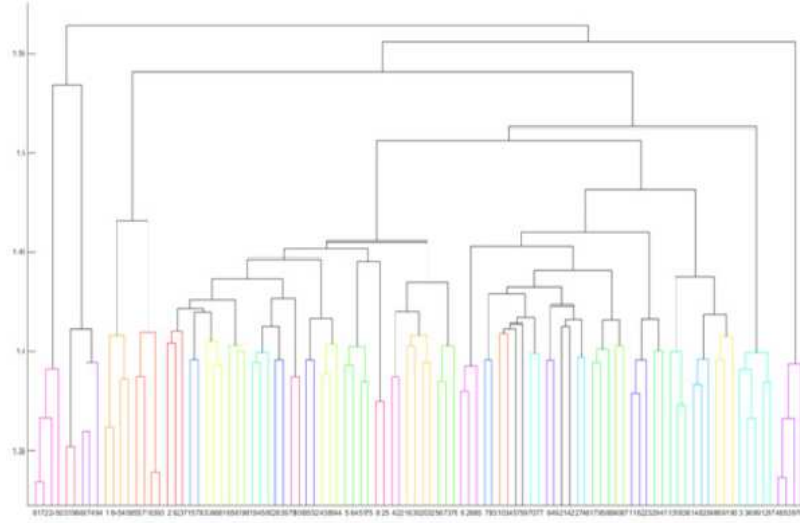
(a) Example of a Dendrogram with 102 Classes of CalTech-101 dataset generated using confusion matrix obtained from a single CNN (Better viewed in color).



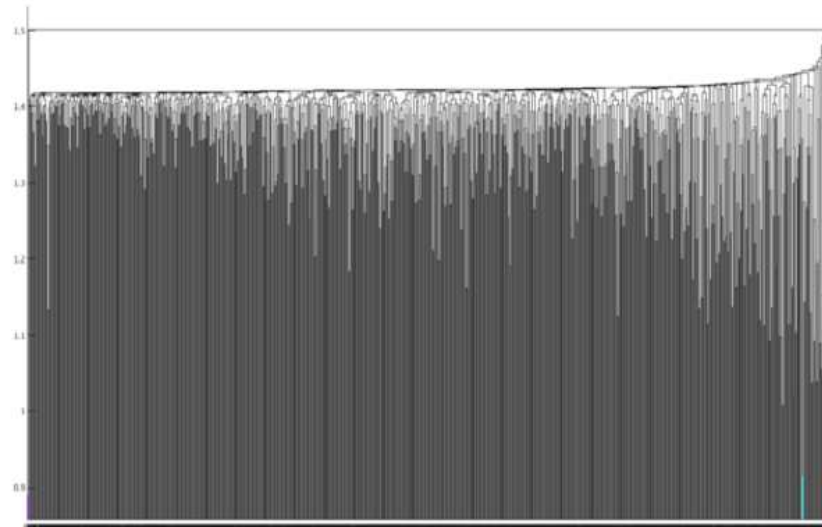
(b) Example of a Dendrogram with 257 Classes of CalTech-256 dataset generated using confusion matrix obtained from a single CNN.

Fig. 6. Examples of Dendrograms for CalTech Datasets

CIFAR-100 dataset also provides a higher level taxonomy. So, we compared the performance of hierarchical models with the original (ground truth) clusters in Table 9. The CIFAR hierarchical model and CIFAR adaptive network selection models are generated using the CIFAR-100 taxonomy. The learned taxonomy improves  $CNN_1$  accuracy by 5.62% where as CIFAR-100 taxonomy improves  $CNN_1$  accuracy by 1.28%. It was observed that our taxonomy generated more clusters, hence finer



(a) Example of a dendrogram with 100 Classes of CIFAR-100 dataset generated using confusion matrix obtained from a single CNN.



(b) Example of a dendrogram with 1000 Classes of ImageNet dataset generated using confusion matrix obtained from a single CNN.

Fig. 7. Examples of a Dendrogram for CIFAR-100 and Imagenet datasets.

categories.

Table 10. lists results on CalTech-101, CalTech-256, and CIFAR-100 datasets.

Table 9. Performance of a single *CNN* compared with models generated from adaptive clustering and ground truth CIFAR-100 taxonomy.

S.No	Model	Clusters	Accuracy(%)
1	$CNN_1$	NA	42.29
2	CIFAR hierarchical model	20	41.82
3	CIFAR adaptive network selection	20	42.83
4	Hierarchical model	30	37.56
5	Adaptive network selection	30	<b>44.67</b>

The non-adaptive hierarchical models and adaptive network selection generally do not improve the performance over a single, large CNN. Adaptive transfer learning experiments improve performance over a single CNN (these were not performed on CIFAR-100 due to the smaller size of the images in the dataset). We assume these variations in performance are due to the data-driven nature of CNNs. Both the CalTech datasets have significant variation in number of samples per class, and the results presented in this study were obtained on the entire dataset. Since CIFAR-100 has sufficient samples per class, class assignment classifiers can optimize network weights, whereas for CalTech-101 and CalTech-256, many class assignment classifiers have very few training samples.

Table 10. Performance comparison of a single *CNN* with hierarchical models.

Dataset	$CNN_1$	Hierarchical model	Adaptive network selection	Adaptive transfer learning	Joint model
CalTech-101	55.12	51.57	53.25	54.85	<b>55.12</b>
CalTech-256	36.21	28.34	29.54	<b>36.65</b>	36.54
CIFAR-100	42.29	37.56	<b>44.67</b>	NA	<b>44.67</b>

We believe the accuracies would be higher if the number of examples were identical across all classes. To validate this assumption, the performance of the non-adaptive hierarchical model as well as adaptive hierarchical models were evaluated on subsets of the ImageNet dataset.

Table 11. Performance comparison of a single CNN with hierarchical model and adaptive transfer learning model on ImageNet dataset.

Model	Clusters	Accuracy (%)
$CNN_{TL_1}$	NA	55.32
Hierarchical model	89	50.27
Adaptive transfer learning	89	<b>56.06</b>

Table 11. demonstrates 1.3% increase in accuracy relatively compared to a single *CNN*. It was observed that some classes in the ImageNet possess extreme similarities and led to formation of clusters with many classes or fine categories. This hinders the performance of hierarchy classifier hurting the overall accuracy. We hypothesize that the hierarchy classifiers performance would be improved if the resulted clusters had an even distribution of classes across them.

### 4.3. Analysis

In order to make the final class prediction, HD-CNN<sup>37</sup> uses a probabilistic averaging layer that takes inputs from all fine category CNNs as well as coarse category CNNs. HD-CNN achieves a lower error at the expense of increased computational complexity. Our models significantly reduce the computations by making final predictions using just one fine category CNN.

Our work aims at lowering the computational complexity while achieving scalability. Although we underperform compared to HD-CNN, our models perform better than their base-line results. The performances of hierarchical models in this work demonstrate the advantages of various hierarchical architectures while improving baseline results, but are not intended to compete with state-of-the-art results. Tables 12 & 13 show the complexity analysis in terms of memory footprint for each network used while testing an image. Table 12. show the memory required by different CNN architectures used in the adaptive transfer learning models to predict the final class. To make comparisons with others, we measure the memory requirements for test mini batch size of 50.

Table 12. Comparison of memory footprint between different CNN architectures used in adaptive transfer learning model.

Network	$CNN_{TL_1}$	$CNN_{TL_2}$	$CNN_{TL_3}$	$CNN_{TL_4}$	$CNN_{TL_5}$
Params Memory (MB)	232.03	169.1	97.1	84.56	48.56
Data Memory $\times$ 50 (MB)	314.5	314	313	312	311
Total Memory (MB)	546.53	483.1	410.1	396.56	359.56

The baseline VGG-f ( $CNN_{TL_1}$ ) model requires 546.53 mega-bytes memory to make a final class estimation. For similar class estimation, the hierarchical classifier requires ( $CNN_{TL_3}$ ) 97.1 mega-bytes and and class assignment classifier ( $CNN_{TL_5}$ ) 48.56 mega-bytes. The hierarchical model shares the data between both stages and requires 313 mega-bytes. Hence, overall the hierarchical model would require  $97.1 + 48.56 + 313 = 458.66$  mega-bytes memory. In case of adaptive transfer learning, it can use any model from  $CNN_{TL_2}$  to  $CNN_{TL_5}$ , so it would require  $97.1 + 169.1 + 314 = 580.2$  mega-bytes in the worst case scenario. Hence, the hierarchical models are expected to use less resources compared to baseline models.

Table 13 shows that memory requirements are approximately  $14 \times$  lower com-

Table 13. Comparison of test accuracy and memory footprint between building block nets, HD-CNNs and hierarchical models on the ImageNet dataset. The testing mini-batch size is 50.

Model	Accuracy (%)	Memory (MB)	Layers
Baseline VGG-f	55.32	546	7
Hierarchical model	50.07	458.66	7
Adaptive transfer learning	56.06	580.2	7
Baseline VGG-16 layer	67.7	4134	16
HD-CNN + CE + PC	68.66	6863	16

pared to the best model of the HD-CNN<sup>37</sup>. We also estimate that our models would require fewer computations while achieving improved performance when visual recognition task is scaled upwards to tens of thousands of object categories.

## 5. Conclusion

An automatic hierarchical clustering method is introduced which reduces parameters while simultaneously increasing classification accuracy. This new approach borrows concepts from traditional divisive clustering techniques as well as confusion matrix dissimilarity linkage tree decomposition, to create an iterative method which methodically identifies cluster boundaries in a natural fashion. Hierarchical cluster boundary formation was tested on both MLP and CNN classifier frameworks, and shows significant benefit to the former, but marginal in the latter. It is hypothesized that other classification frameworks such as SVM and Bayes classifiers can also benefit from the hierarchical framework. What is most intriguing is that the proposed strategy allows for virtually unlimited number of classes in any particular classification problem.

The proposed adaptive network selection framework, consisting of hierarchical models based on adaptive transfer learning, outperform single CNN models. The class assignment classifier network configuration is based on class confusion and composition statistics. As the complexity of classification problems increase, hierarchical models will offer significant benefits for large scale classification problems. Future work will demonstrate adaptive hierarchical clustering over multiple stages on the full ImageNet-22K dataset. Use of ensembles to improve hierarchical classifier accuracy, data augmentations on imbalanced cluster to eradicate biases in hierarchical classifier predictions, and sharing initial layers among the class assignment classifiers will be used to improve hierarchical framework performance.

## Acknowledgments

We acknowledge NVIDIA for providing some of the GPU computing resources used in this research. We also thank Karthik Veerabhadra for his help in running some experiments.

## References

1. H. Bay, A. Ess, T. Tuytelaars and L. Van Gool, Speeded-up robust features (SURF), *Computer vision and image understanding* **110**(3) (2008) 346–359.
2. N. Dalal and B. Triggs, Histograms of oriented gradients for human detection, in *Computer Vision and Pattern Recognition, 2005. CVPR 2005. IEEE Computer Society Conference on*, Vol. 1 (2005) pp. 886–893.
3. T. Dean, M. Ruzon, M. Segal, J. Shlens, S. Vijayanarasimhan and J. Yagnik, Fast, accurate detection of 100,000 object classes on a single machine, in *Proceedings of the IEEE Conference on Computer Vision and Pattern Recognition* (2013) pp. 1814–1821.
4. J. Deng, N. Ding, Y. Jia, A. Frome, K. Murphy, S. Bengio, Y. Li, H. Neven and H. Adam, Computer Vision – ECCV 2014: 13th European Conference, Zurich, Switzerland, September 6–12, 2014, Proceedings, Part I (Springer International Publishing, Cham, 2014) pp. 48–64.
5. J. Deng, W. Dong, R. Socher, L.-J. Li, K. Li and L. Fei-Fei, Imagenet: A large-scale hierarchical image database, in *Computer Vision and Pattern Recognition, 2009. CVPR 2009. IEEE Conference on* (2009) pp. 248–255.
6. L. Fei-Fei, R. Fergus and P. Perona, Learning generative visual models from few training examples: An incremental bayesian approach tested on 101 object categories, *Computer Vision and Image Understanding* **106**(1) (2007) 59–70.
7. S. Godbole, Exploiting confusion matrices for automatic generation of topic hierarchies and scaling up multi-way classifiers, *Progress Report, IIT Bombay* (MARCH 2002) (2002) p. 17.
8. I. J. Goodfellow, D. Warde-Farley, M. Mirza, A. Courville and Y. Bengio, Maxout networks, *arXiv preprint arXiv:1302.4389* (2013).
9. K. He, X. Zhang, S. Ren and J. Sun, Deep Residual Learning for Image Recognition, *arXiv preprint arXiv:1512.03385* (2015).
10. K. He, X. Zhang, S. Ren and J. Sun, Delving deep into rectifiers: Surpassing human-level performance on imagenet classification, in *Proceedings of the IEEE International Conference on Computer Vision* (2015) pp. 1026–1034.
11. K. He, X. Zhang, S. Ren and J. Sun, Spatial pyramid pooling in deep convolutional networks for visual recognition, *Pattern Analysis and Machine Intelligence, IEEE Transactions on* **37**(9) (2015) 1904–1916.
12. G. E. Hinton, N. Srivastava, A. Krizhevsky, I. Sutskever and R. R. Salakhutdinov, Improving neural networks by preventing co-adaptation of feature detectors, *arXiv preprint arXiv:1207.0580* (2012).
13. J. Hoffman, S. Guadarrama, E. S. Tzeng, R. Hu, J. Donahue, R. Girshick, T. Darrell and K. Saenko, LSDA: Large scale detection through adaptation, in *Advances in Neural Information Processing Systems* (2014) pp. 3536–3544.
14. A. G. Howard, Some improvements on deep convolutional neural network based image classification, *arXiv preprint arXiv:1312.5402* (2013).
15. D. H. Hubel and T. N. Wiesel, Receptive fields and functional architecture of monkey striate cortex, *The Journal of Physiology* **195**(1) (1968) 215–243.
16. A. Krizhevsky, I. Sutskever and G. E. Hinton, Imagenet classification with deep convolutional neural networks, in *Advances in neural information processing systems* (2012) pp. 1097–1105.
17. N. Kruger, P. Janssen, S. Kalkan, M. Lappe, A. Leonardis, J. Piater, A. J. Rodriguez-Sanchez and L. Wiskott, Deep hierarchies in the primate visual cortex: What can we learn for computer vision?, *Pattern Analysis and Machine Intelligence, IEEE Transactions on* **35**(8) (2013) 1847–1871.
18. Y. LeCun, L. Bottou, Y. Bengio and P. Haffner, Gradient Based Learning Applied to

- Document Recognition, *Proceedings of the IEEE* **86**(11) (1998) 2278–2324.
19. M. Lin, Q. Chen and S. Yan, Network in network, *arXiv preprint arXiv:1312.4400* (2013).
  20. D. G. Lowe, Distinctive image features from scale-invariant keypoints, *International journal of computer vision* **60**(2) (2004) 91–110.
  21. A. L. Maas, A. Y. Hannun and A. Y. Ng, Rectifier nonlinearities improve neural network acoustic models, in *Proc. ICML*, Vol. 30 (2013) p. 1.
  22. A.-r. Mohamed, G. E. Dahl and G. Hinton, Acoustic modeling using deep belief networks, *Audio, Speech, and Language Processing, IEEE Transactions on* **20**(1) (2012) 14–22.
  23. V. Nair and G. E. Hinton, Rectified linear units improve restricted boltzmann machines, in *Proceedings of the 27th International Conference on Machine Learning (ICML-10)* (2010) pp. 807–814.
  24. I. T. Podolak, Hierarchical classifier with overlapping class groups, *Expert Systems with Applications* **34**(1) (2008) 673–682.
  25. O. Russakovsky, J. Deng, H. Su, J. Krause, S. Satheesh, S. Ma, Z. Huang, A. Karpathy, A. Khosla, M. Bernstein and others, Imagenet large scale visual recognition challenge, 2014, *arXiv preprint arXiv:1409.0575*.
  26. R. Salakhutdinov, J. B. Tenenbaum and A. Torralba, Learning with hierarchical-deep models, *Pattern Analysis and Machine Intelligence, IEEE Transactions on* **35**(8) (2013) 1958–1971.
  27. K. Simonyan and A. Zisserman, Very deep convolutional networks for large-scale image recognition, *Iclr* (2015) 1–14.
  28. N. Srivastava, G. Hinton, A. Krizhevsky, I. Sutskever and R. Salakhutdinov, Dropout: A simple way to prevent neural networks from overfitting, *The Journal of Machine Learning Research* **15**(1) (2014) 1929–1958.
  29. N. Srivastava and R. R. Salakhutdinov, Discriminative Transfer Learning with Tree-based Priors, in C. J. C. Burges, L. Bottou, M. Welling, Z. Ghahramani and K. Q. Weinberger (eds.), *Advances in Neural Information Processing Systems 26* (Curran Associates, Inc., 2013) pp. 2094–2102.
  30. R. K. Srivastava, J. Masci, S. Kazerounian, F. Gomez and J. Schmidhuber, Compete to compute, in *Advances in Neural Information Processing Systems* (2013) pp. 2310–2318.
  31. C. Szegedy, S. Ioffe and V. Vanhoucke, Inception-v4, inception-resnet and the impact of residual connections on learning, *arXiv preprint arXiv:1602.07261* (2016).
  32. C. Szegedy, P. Sermanet, S. Reed, D. Anguelov, D. Erhan, V. Vanhoucke and A. Rabinovich, Going deeper with convolutions, *2015 IEEE Conference on Computer Vision and Pattern Recognition (CVPR)* (2015) 1–9.
  33. A.-M. Tousch, S. Herbin and J.-Y. Audibert, Semantic hierarchies for image annotation: A survey, *Pattern Recognition* **45**(1) (2012) 333–345.
  34. L. Wan, M. Zeiler, S. Zhang, Y. L. Cun and R. Fergus, Regularization of neural networks using dropconnect, in *Proceedings of the 30th International Conference on Machine Learning (ICML-13)* (2013) pp. 1058–1066.
  35. T. Xiao, J. Zhang, K. Yang, Y. Peng and Z. Zhang, Error-Driven Incremental Learning in Deep Convolutional Neural Network for Large-Scale Image Classification, in *Proceedings of the 22Nd ACM International Conference on Multimedia, MM '14* (ACM, New York, NY, USA, 2014) pp. 177–186.
  36. Y. Xiong, Building text hierarchical structure by using confusion matrix, in *2012 5th International Conference on BioMedical Engineering and Informatics* (2012)
  37. Z. Yan, H. Zhang, R. Piramuthu, V. Jagadeesh, D. DeCoste, W. Di and Y. Yu,

HD-CNN: Hierarchical Deep Convolutional Neural Network for Large Scale Visual Recognition (2014) 1–13.

38. M. D. Zeiler and R. Fergus, Visualizing and understanding convolutional networks, in *Computer vision–ECCV 2014* (Springer, 2014) pp. 818–833.
39. A. Zisserman, The pascal visual object classes (voc) challenge, *International Journal of Computer Vision* **88**(2) (2010) p. 303338.

## Appendix A. Appendices

Table 14, Table 15 & Table 16 shows the estimation of parameter memory and data memory required by  $CNN_{TL_1}$ ,  $CNN_{TL_3}$  and  $CNN_{TL_5}$  to make prediction on a test image.

Table 14. Memory requirements for a Single CNN to make final prediction on a test image.

ImageNet: Single CNN Classifier $CNN_{TL_1}$ . MEMORY: 238.32 MB										
Layer	Function					Data Memory (MB)				Params Memory (MB)
0	Input	224	224	3	0.57	0	0	0	0	0
1	Conv1	54	54	64	0.71	11	11	3	64	0.09
1	ReLU1	54	54	64	0.71	0	0	0	0	0
1	norm1	54	54	64	0.71	0	0	0	0	0
1	Pool1	27	27	64	0.18	0	0	0	0	0
2	Conv2	27	27	256	0.71	5	5	64	256	1.56
2	ReLU2	27	27	256	0.71	0	0	0	0	0
2	norm2	27	27	256	0.71	0	0	0	0	0
2	Pool2	13	13	256	0.17	0	0	0	0	0
3	Conv3	13	13	256	0.17	3	3	256	256	2.25
3	ReLU3	13	13	256	0.17	0	0	0	0	0
4	Conv4	13	13	256	0.17	3	3	256	256	2.25
4	ReLU4	13	13	256	0.17	0	0	0	0	0
5	Conv5	13	13	256	0.17	3	3	256	256	2.25
5	ReLU5	13	13	256	0.17	0	0	0	0	0
5	Pool5	6	6	256	0.04	0	0	0	0	0
6	Fc6	1	1	4096	0.02	6	6	256	4096	144
6	ReLU6	1	1	4096	0.02	0	0	0	0	0
7	Fc7	1	1	4096	0.02	1	1	4096	4096	64
7	ReLU7	1	1	4096	0.02	0	0	0	0	0
8	prob	1	1	1000	0.01	1	1	4096	1000	15.63
Total		6.29								232.03



Table 15. Memory requirements for a hierarchy classifier to make coarse category prediction on a test image

ImageNet: hierarchy classifier $CNN_{TL_3}$ . MEMORY: 103.36 MB										
Layer	Function					Data Memory (MB)				Params Memory (MB)
0	Input	224	224	3	0.57	0	0	0	0	0
1	Conv1	54	54	64	0.71	11	11	3	64	0.09
1	ReLU1	54	54	64	0.71	0	0	0	0	0
1	norm1	54	54	64	0.71	0	0	0	0	0
1	Pool1	27	27	64	0.18	0	0	0	0	0
2	Conv2	27	27	256	0.71	5	5	64	256	1.56
2	ReLU2	27	27	256	0.71	0	0	0	0	0
2	norm2	27	27	256	0.71	0	0	0	0	0
2	Pool2	13	13	256	0.17	0	0	0	0	0
3	Conv3	13	13	256	0.17	3	3	256	256	2.25
3	ReLU3	13	13	256	0.17	0	0	0	0	0
4	Conv4	13	13	256	0.17	3	3	256	256	2.25
4	ReLU4	13	13	256	0.17	0	0	0	0	0
5	Conv5	13	13	256	0.17	3	3	256	256	2.25
5	ReLU5	13	13	256	0.17	0	0	0	0	0
5	Pool5	6	6	256	0.04	0	0	0	0	0
6	Fc6	1	1	2048	0.01	6	6	256	2048	72
6	ReLU6	1	1	2048	0.01	0	0	0	0	0
7	Fc7	1	1	2048	0.01	1	1	2048	2048	16
7	ReLU7	1	1	2048	0.01	0	0	0	0	0.
8	prob	1	1	89	0.01	1	1	2048	89	0.7
Total						6.26				97.1

Table 16. Memory requirements for a class assignment classifier to make fine category prediction on a test image.

**ImageNet: class assignment classifier  $CNN_{TL_5}$ . MEMORY: 54.84 MB (Worst Case )**

Layer	Function					Data Memory (MB)				Params Memory (MB)
0	Input	224	224	3	0.57	0	0	0	0	0
1	Conv1	54	54	64	0.71	11	11	3	64	0.09
1	ReLU1	54	54	64	0.71	0	0	0	0	0
1	norm1	54	54	64	0.71	0	0	0	0	0
1	Pool1	27	27	64	0.18	0	0	0	0	0
2	Conv2	27	27	256	0.71	5	5	64	256	1.56
2	ReLU2	27	27	256	0.71	0	0	0	0	0
2	norm2	27	27	256	0.71	0	0	0	0	0
2	Pool2	13	13	256	0.17	0	0	0	0	0
3	Conv3	13	13	256	0.17	3	3	256	256	2.25
3	ReLU3	13	13	256	0.17	0	0	0	0	0
4	Conv4	13	13	256	0.17	3	3	256	256	2.25
4	ReLU4	13	13	256	0.17	0	0	0	0	0
5	Conv5	13	13	256	0.17	3	3	256	256	2.25
5	ReLU5	13	13	256	0.17	0	0	0	0	0
5	Pool5	6	6	256	0.04	0	0	0	0	0
6	Fc6	1	1	1024	0.01	6	6	256	1024	36
6	ReLU6	1	1	1024	0.01	0	0	0	0	0
7	Fc7	1	1	1024	0.01	1	1	1024	1024	4
7	ReLU7	1	1	1024	0.01	0	0	0	0	0
8	prob	1	1	41	0.01	1	1	1024	41	0.16
<b>Total</b>						<b>6.26</b>				<b>48.56</b>

*Note:* Worst case indicates a network predicting classes in a cluster with maximum number of classes.